Original Paper

Preparation of glass-ceramics with needle-like apatite crystals of different aspect ratios and their behavior during extrusion[1)]

Cornelia Moisescu, Gunter Carl and Christian Rüssel

Otto-Schott-Institut für Glaschemie, Friedrich-Schiller-Universität, Jena (Germany)

Glass-ceramics containing needle-like apatite crystals were produced from glasses in the system $SiO_2-Al_2O_3-CaO-P_2O_5-K_2O-F^-$. Crystallization was achieved by rapid heating to 1200 °C and keeping the sample for 0.5 to 15 h. With increasing time of heat treatment, length, L, width, W, as well as the aspect ratio, L/W, of the apatite crystals increased. This also led to an increase in the Newtonian viscosity. At higher shear rates, non-Newtonian flow behavior was observed. This effect was more pronounced with increasing aspect ratio. In all cases, the result of the extrusion process was highly oriented glass-ceramics, if it was carried out in the non-Newtonian range.

Herstellung von Glaskeramiken mit nadelförmigen Apatitkristallen verschiedener Aspektverhältnisse und ihr Verhalten bei der Extrusion

Aus Gläsern im System $SiO_2-Al_2O_3-CaO-P_2O_5-K_2O-F^-$ wurden Glaskeramiken mit nadelförmigen Apatitkristallen hergestellt. Die Kristallisation wurde durch schnelles Aufheizen auf 1200 °C und Haltezeiten im Bereich von 0,5 bis 15 h herbeigeführt. Mit steigender Haltezeit nahmen die Länge L, die Breite W, aber auch das Aspektverhältnis (L/W) der Apatitkristalle zu. Dies führte auch zu einem Ansteigen der Newtonschen Viskosität. Bei höheren Scherraten wurde auch nicht-Newtonsches Fließverhalten, das mit steigendem Aspektverhältnis immer ausgeprägter wurde, beobachtet. In allen Fällen wurden durch den Extrusionsprozeß gut orientierte Glaskeramiken erhalten, falls dieser im nicht-Newtonschen Bereich durchgeführt wurde.

1. Introduction

In the past few years, numerous studies on the preparation of oriented glass-ceramics by means of extrusion have been reported [1 to 5]. Here, usually a glass melt containing anisometric crystals, i. e. of needle-like or plate-like morphology, is used. Due to the plastic deformation process, orientation is achieved by the high shear stresses applied. In a recent paper [4], it was pointed out that the extrusion process can also be utilized to study the rheological behavior of a melt, especially in a viscosity range of 10^7 to 10^9 dPa s. In a calcium metaphosphate melt, it has been shown that also non-Newtonian flow, achieved by the alignment of metaphosphate chain structures, can be analyzed at high shear stresses applied. This alignment has also been proved by rotorsynchronized NMR spectroscopy [6].

Received 21 December 1999, revised manuscript 1 March 2000.

[1)] Presented in German as poster at: 73rd Annual Meeting of the German Society of Glass Technology (DGG) in Halle (Germany) on 31 May to 2 June 1999.

The dependence of Newtonian flow upon the quantity of crystalline phase suspended was reported in [7]. Furthermore, the effect of crystal size and shape on Newtonian flow was studied [8]. The occurrence of shear stress may also induce nucleation as shown in the case of lithium disilicate melts [9]. This effect was explained to be caused by shear thinning, i. e. the decrease in viscosity at the shear stress applied. Generally, non-Newtonian flow behavior may be observed in glass melts [10, 7, 10 to 12] at high shear stresses. This effect is especially observed in glass melts with chain structure and reported to be caused by the alignment of flow units [13 to 17]. In partially crystalline melt, an additional effect contributing to non-Newtonian flow is the alignment of anisometric crystals [15 and 18]. In [18] it was shown that also the non-Newtonian flow behavior is an effect of the shape of the crystals suspended in the melt. If they possess isometric shape, non-Newtonian flow may solely be caused by the glassy phase, i. e. the formation of anisometric flow units. Then the shear stresses, necessary to induce non-Newtonian flow, are fairly high. If, however, the crystals are anisometric, their alignment

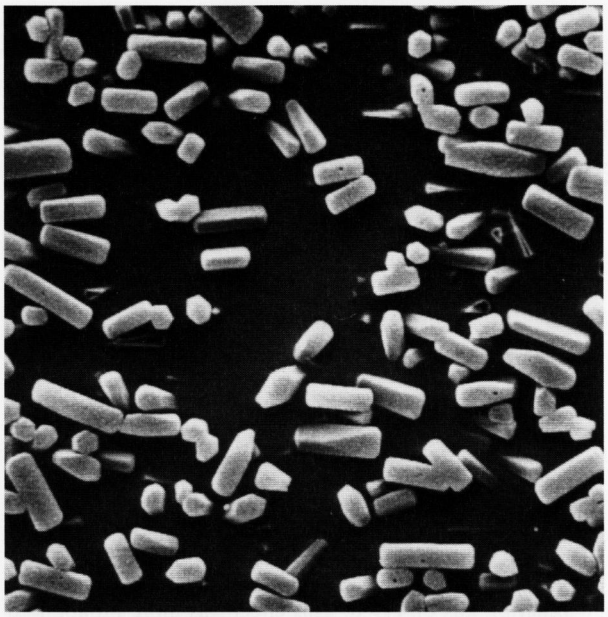

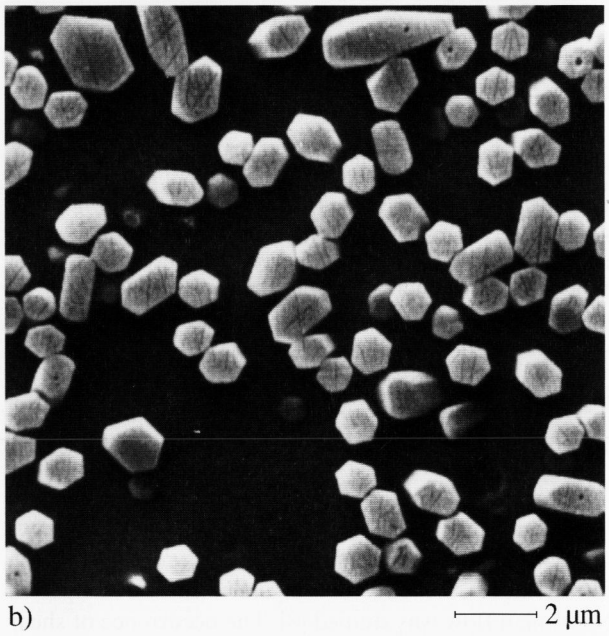

Figures 1a and b. SEM micrographs of extruded samples thermally pretreated at 1200 °C for 0.5 h; a) cut parallel, b) cut perpendicularly to the extrusion direction (piston velocity: 2 mm/min).

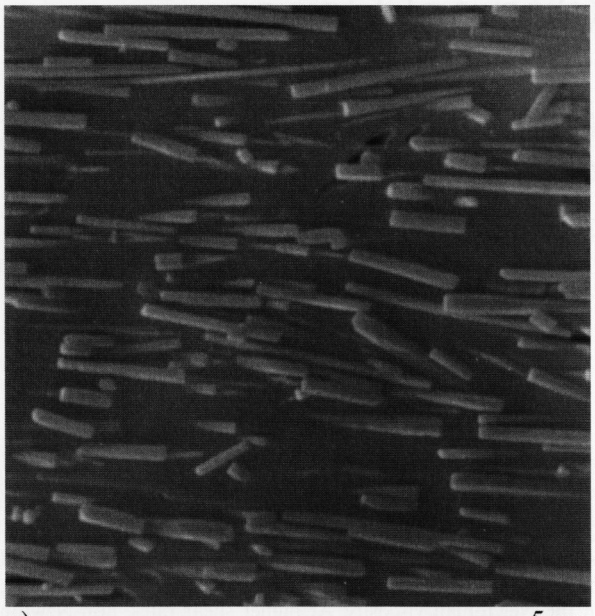

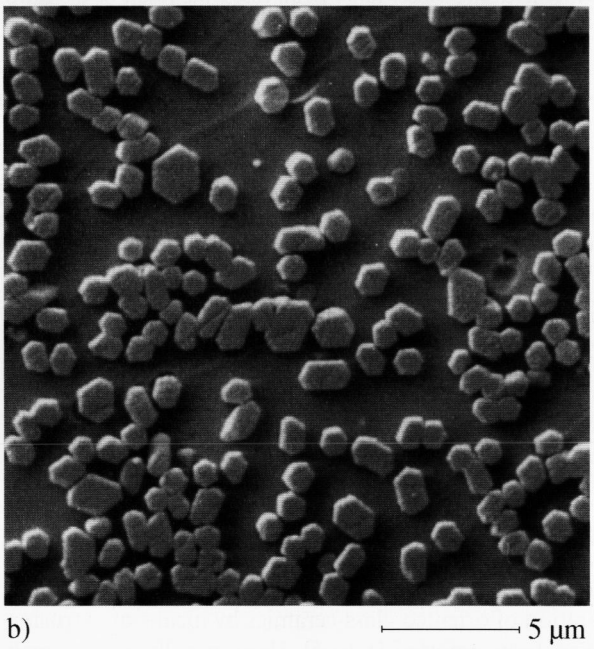

Figures 2a and b. SEM micrographs of extruded samples thermally pretreated at 1200 °C for 1 h; a) cut parallel, b) cut perpendicularly to the extrusion direction (piston velocity: 2 mm/min).

and hence non-Newtonian flow occurs at much lower shear stress. This paper provides a study on both the Newtonian and the non-Newtonian flow of a glass melt containing needle-like fluoroapatite crystals of different size and aspect ratio (length: width).

2. Experimental

A glass with the composition (in mol%) of 22.5 SiO_2, 20.1 Al_2O_3, 18.1 CaO, 22.8 P_2O_5, 9.2 K_2O and 7.3 F^- was melted from reagent grade raw materials in an alumina crucible at 1500 °C, cast in water and crushed. The glass was remelted in a platinum crucible at 1500 °C and cast in a graphite mold. During cooling partial crystallization occurred. The crystal phase formed was fluoroapatite. These glass-ceramics were put into a furnace preheated to 1200 °C and soaked for 0.5 to 15 h. After thermal treatment, the glass-ceramics were inserted into an extrusion chamber, already described in [1, 17 and 19]. The experiment was carried out using a ZWICK-Universal Testing Machine 1445 (Zwick GmbH & Co., Ulm (Germany)), controlled by a computer. The piston

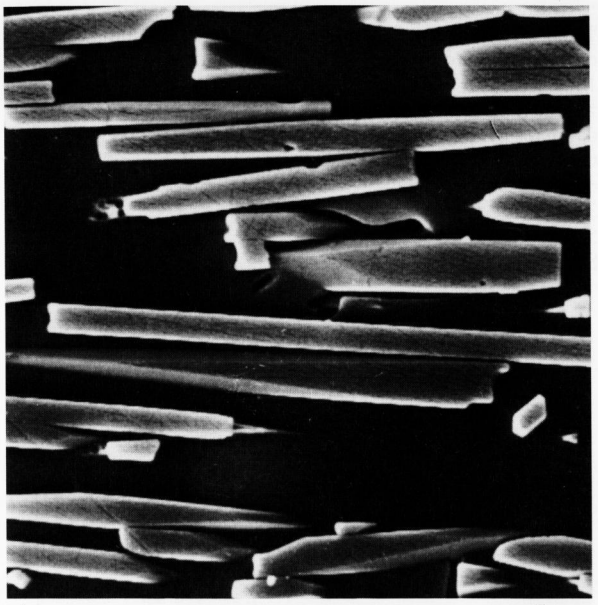

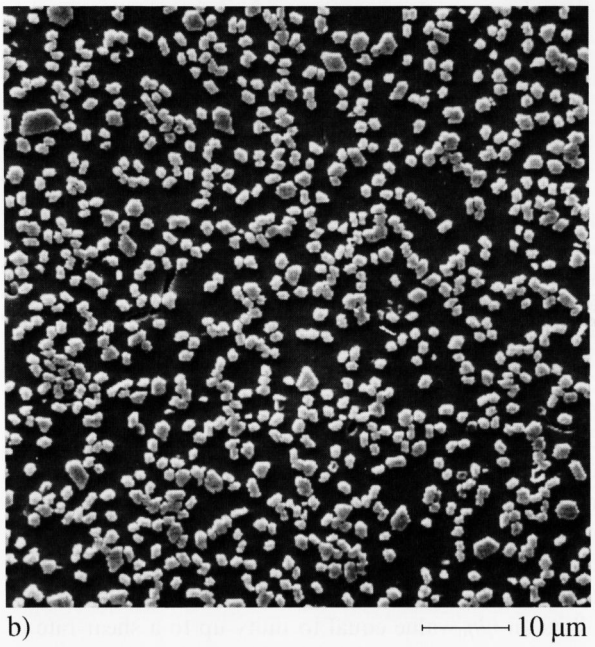

Figures 3a and b. SEM micrographs of extruded samples thermally pretreated at 1200 °C for 15 h; a) cut parallel, b) cut perpendicularly to the extrusion direction (piston velocity: 2 mm/min).

(diameter: 21.6 mm) was driven by an electric motor, the piston velocity was in the range of 0.2 to 2 mm/min. The extrusion chamber was located in a furnace maintaining a temperature of 700 °C. Extrusion was carried out with cylindrical graphite dies possessing diameters of 3, 5 and 8 mm. The temperature at the exit of the extrusion orifice was measured by a thermocouple. The extrusion principle and the procedure applied have already been described in detail by Roeder et al. [19]. During extrusion the load was controlled in such a manner that the extrusion velocity remained constant and was equal

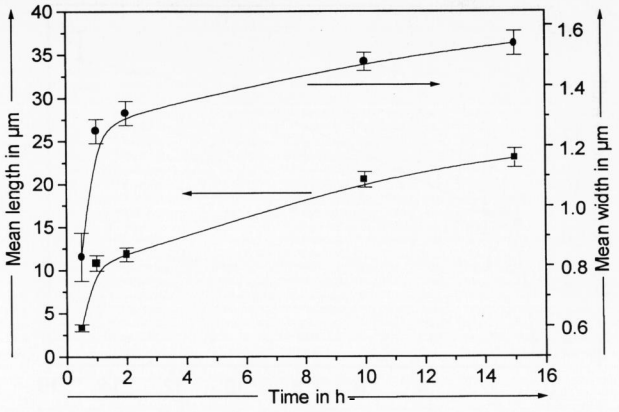

Figure 4. Mean lengths and widths of the apatite crystals in extruded samples as a function of the time of thermal pretreatment at 1200 °C.

to the preset value. Extruded rods were cut parallel and perpendicularly to the extrusion direction and characterized by X-ray diffraction (XRD) (Siemens D 5000, Siemens AG, München (Germany)) and scanning electron microscopy (SEM) (DSM 940 A, Carl Zeiss, Oberkochen (Germany)). Lengths, widths and aspect ratios were determined by an automatic image analyzer (Zeiss Optimas).

3. Results

Figures 1a and b, 2a and b, 3a and b present SEM micrographs of extruded samples. They were cut parallel (figures a) and perpendicularly (figures b) to the extrusion direction. In figure 1a elongated crystals are observed which preferably are oriented in the extrusion direction. This sample was soaked for 0.5 h at 1200 °C. The mean length of the crystals was (3.3 ± 0.4) µm. The mean width (0.83 ± 0.08) µm was determined from figure 1b. Figures 2a and b and 3a and b are attributed to samples soaked at 1200 °C for 1 and 15 h, respectively. Here, the crystals are more elongated and of needle-like shape. The mean lengths are (10.8 ± 0.9) and (23 ± 1.1) µm, respectively. During soaking the widths increased from (0.83 to 1.25 ± 0.04) and (1.54 ± 0.04) µm for soaking times of 0.5, 1 and 15 h, respectively. Crystal dimensions, including those of samples extruded after supplying other soaking times, are summarized in figure 4. A steady increase in the lengths and widths is observed. Within the time from 0.5 to 15 h, the crystals increased in length by the factor of seven, while the increase in width is much smaller (factor 1.86). In figure 5, the aspect ratio is shown. During thermal pretreatment, it increases from 4 : 1 to 14.9 : 1.

Figure 6 shows viscosities calculated using equation 1 [20 and 21] as a function of the aspect ratio.

$$\eta \equiv F/[2\,\pi\,v\,D_0\,((D_0/D_1)^3-1)] \qquad (1)$$

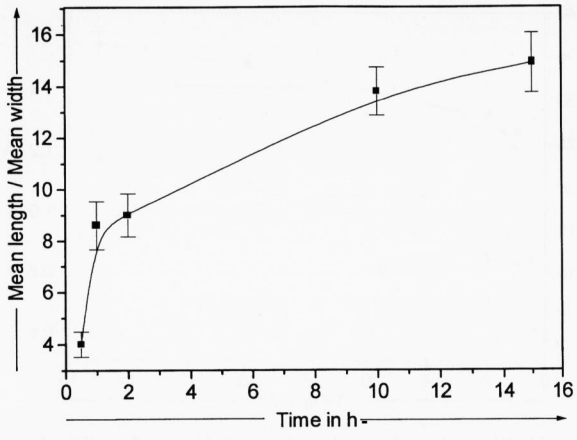

Figure 5. Aspect ratios of the apatite crystals calculated from figure 4 as a function of the time of thermal pretreatment at 1200 °C.

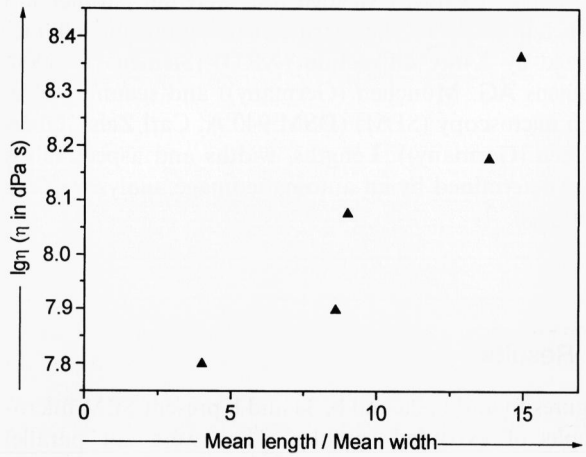

Figure 6. Viscosities as a function of the aspect ratio of the apatite crystals at a piston velocity of 2 mm/min.

with D_0 = diameter of the container chamber, D_1 = diameter of the die, v = piston velocity, F = load.

During the experiments, a piston velocity of 2 mm/min was supplied. It is observed that the viscosity calculated increases with increasing aspect ratio. At an aspect ratio of 4 : 1, the viscosity is by around the factor of 3.5 lower than in a sample possessing an aspect ratio of 14.9 : 1.

Table 1 presents viscosities measured using different die diameters. They were varied from 3 to 5 and 8 mm, resulting in pressing ratios of 51.4, 18.5 and 7.22. The viscosities calculated from the load necessary to maintain the present piston velocity of 0.5 mm/min varied with the pressing ratio. For the largest die diameter of 8 mm, viscosity was highest ($33.6 \cdot 10^7$ dPa s), while it was lowest for the smallest die diameter ($6 \cdot 10^7$ dPa s). The viscosity for the medium size die (5 mm) lay in between.

Table 1. Diameters of the die, pressing ratio used and viscosities calculated; piston velocity: 0.5 mm/s, soaking time at 1200 °C: 1 h

diameter of the die in mm	pressing ratio	viscosity in 10^7 dPa s
3	51.4	6
5	18.5	9.4
8	7.22	33.6

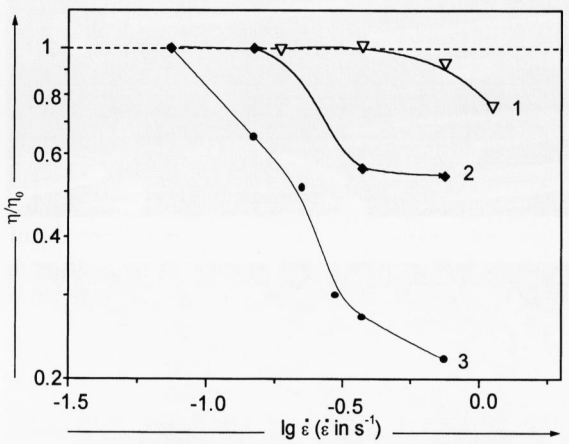

Figure 7. Normalized viscosities as a function of the shear rate applied. Curve 1: sample as cast from the melt without thermal treatment, curve 2: sample heat-treated for 30 min, curve 3: sample heat-treated for 15 h.

Figure 7 shows viscosities measured at different shear rates applied. While curve 1 is attributed to a glass-ceramic without any thermal pretreatment, curves 2 and 3 were recorded from glass-ceramics tempered at 1200 °C for 0.5 and 15 h, respectively. The curves were normalized to viscosities measured at low shear rate. While curve 1 exhibits an η/η_0 value equal to unity up to a shear rate of 0.4 s^{-1}, in curves 2 and 3 values lower than 1 are already observed at shear rates of 0.4 and 0.15 s^{-1}, respectively. It should be noted that apatite crystals are approximately spherical in the glass without thermal treatment (curve 1), and exhibit aspect ratios of 4 : 1 and 14.9 : 1 (curves 2 and 3) for samples tempered for 0.5 and 15 h. Hence, it is seen that normalized viscosities lower than one are observed at decreasing shear rates, if the aspect ratio of the crystals suspended increases.

4. Discussion

As shown in figures 1a and b, 2a and b, 3a and b and 4, both lengths and widths of the crystals formed increase with increasing time of thermal treatment. According to the theory of crystal growth [22] for the stage

of crystal coarsening, a dependence of the crystal size, d, upon the time of heat treatment, according to a $t^{1/3}$ law is expected (Ostwald ripening):

$$d \sim t^{1/3}. \quad (2)$$

In figure 8, a plot of both crystal lengths and widths against $t^{1/3}$ is shown. For times in the range of 1 to 15 h, within the error limits, a linear correlation is observed. Hence, in this range the growth behavior can be fitted to equation (2). This equation was derived assuming that first, the total content of the crystalline phase is constant and second, the driving force for crystal growth is the minimization of surface energy while third, the transport is solely achieved by diffusion. Width and length after tempering for 0.5 h are not in agreement with the $t^{1/3}$ law. It should be assumed that after 0.5 h, the quantity of apatite phase is still changing and hence the prerequisites for Ostwald ripening are not fulfilled. The strongly anisotropic growth of the crystals might be caused by very different surface tensions in different crystallographic directions or by a growth mechanism not solely controlled by diffusion. In the latter case, the impingement rate depends on the crystallographic direction, e. g., caused by different densities of screw dislocations along which crystal growth more easily occurs. At the moment, we cannot decide which mechanism is predominant, however, it will be a subject of future studies. The different growth rates in different crystallographic directions – the long axis is the crystallographic c axis – leads to an increase in the aspect ratio of the crystals with time as shown in figure 5. Hence, the morphology occurring can be controlled by the time of heat treatment at 1200 °C.

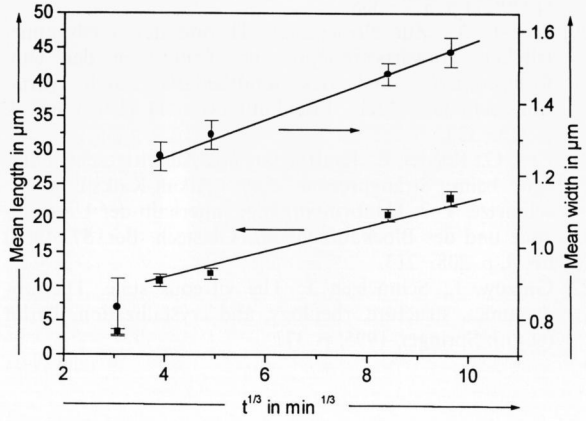

Figure 8. Mean lengths and widths of the apatite crystals as a function of $t^{1/3}$.

Lenghts and widths of the crystals were determined after extrusion of the partially crystalline sample. During extrusion, i. e., at the conditions applied (700 °C), further crystal growth was not observed. After extrusion, the quantitative determination of crystal lengths and widths is much easier than in non-extruded samples, because most crystals are oriented along their c axes in the extrusion direction.

As shown in table 1, the viscosity depends on the diameter of the die used during extrusion (D_1) and hence, on the pressing ratio. By using smaller dies, the shear rate increases and hence a higher load is necessary to maintain the piston velocity. However, loads necessary are much lower than expected assuming Newtonian flow behavior. Obviously shear thinning occurs. This is illustrated in more detail in figure 7. In the isometric sample (see curve 1), Newtonian flow behavior is observed up to a shear rate of 0.4 s^{-1}. At higher shear rates, the viscosity slightly decreases and reaches a value of around 75 % of the Newtonian viscosity, η_0, at a shear rate of 1.25 s^{-1}. By contrast, in a sample tempered for 30 min at 1200 °C, flow behavior is Newtonian up to a shear rate of 0.15 s^{-1}. Here, supplying a shear rate of 0.4 s^{-1} leads to non-Newtonian behavior. The observed viscosity is only 56 % of the Newtonian viscosity. In curve 3, attributed to a melt thermally pretreated for 15 h at 1200 °C, first deviations are already observed at a shear rate smaller than 0.15 s^{-1}. In the isometric sample, non-Newtonian flow might solely be caused by the melt itself, i. e., by the alignment of structural units (e. g. chain structures). A contribution of crystal alignment is not possible, because of the approximately spherical shape. The sample attributed to curve 2 exhibits an aspect ratio of 4 : 1. Obviously, this is sufficient to achieve non-Newtonian flow already at shear rates of 0.4 s^{-1}. At an aspect ratio as high as 14.9 : 1 (see curve 3), non-Newtonian effects are much better pronounced: first deviations from Newtonian flow are observed at lower shear rates and the effect of shear rate on viscosity is larger. At a shear rate of 0.5 s^{-1}, η/η_0 is around 0.23, while it is 0.56 in curve 2. As shown in figures 1a and b, 2a and b and 3a and b, during extrusion orientation of the anisometric crystals is achieved. The origin of the non-Newtonian flow observed in figure 7, curves 2 and 3, therefore, has to be seen in the alignment of the anisometric crystals. Obviously, the non-Newtonian effects are better pronounced if the aspect ratio is higher and hence, orientation of the crystals is more easily achieved. Viscosities in figure 6 are measured at a constant piston velocity of 2 mm/min attributed to a shear rate of 0.5 s^{-1}. Here, it is seen that the viscosity measured increases with increasing aspect ratio. Within the range studied, the viscosity increases by the factor of 3.5. At the shear stress applied, all samples shown in figure 6 exhibit non-Newtonian flow behavior. This effect, as already mentioned, is the higher pronounced, the higher the shear stress applied. The effect of non-Newtonian flow is comparably small at an aspect ratio of 4 : 1 ($\eta/\eta_0 = 0.75$) while it is notably higher at an aspect ratio of 14.9 : 1 ($\eta/\eta_0 = 0.23$). However, as seen in figure 6, the viscosities at a piston velocity of 2 mm/min increase with

increasing aspect ratio. Hence, two effects are superimposed: a) the Newtonian viscosity increases with increasing aspect ratio and b) the decrease in viscosity due to the alignment of anisometric crystals gets larger with increasing aspect ratio. Obviously, under the conditions applied, the increase in Newtonian viscosity over-compensates the decrease in viscosity due to non-Newtonian effects while increasing the aspect ratio.

5. Conclusions

The observation that non-Newtonian flow occurs after a certain shear stress is exceeded offers the possibility of estimating the orientation crystals will exhibit after extrusion. While increasing the shear rate, the viscosity drops to smaller values and hence non-Newtonian flow occurs. This decrease in flow resistance is caused by the crystal orientation occurring. At smaller shear rates, Newtonian flow occurs and the extent of crystal alignment will be small or negligible.

*

This work was supported by the Deutsche Forschungsgemeinschaft (DFG), Bonn-Bad Godesberg (Germany).

6. References

[1] Durschang, B. R.; Carl, G.; Rüssel, C. et al.: Glass-ceramic with preferred orientation of $Li_2Si_2O_5$ crystals produced by extrusion below crystallization temperature and subsequent heat treatment. Glastech. Ber. Glass Sci. Technol. **67** (1994) no. 6, p. 171–177.

[2] Habelitz, S.; Carl, G.; Rüssel, C. et al.: Mechanical properties of oriented mica glass ceramic. J. Non-Cryst. Solids **220** (1997) p. 291–298.

[3] Rüssel, C.: Oriented crystallization of glass. A review. J. Non-Cryst. Solids **219** (1997) p. 212–218.

[4] Moisescu, C.; Jana, C.; Habelitz, S. et al.: Oriented fluoroapatite glass-ceramics. J. Non-Cryst. Solids **248** (1999) p. 176–182.

[5] Habelitz, S.; Carl, G.; Rüssel, C. et al.: Oriented mica glass-ceramic by extrusion and subsequent heat treatment. Glastech. Ber. Glass Sci. Technol. **70** (1997) no. 3, p. 86–92.

[6] Braun, M.; Yue, Y.; Rüssel, C. et al.: Two-dimensional nuclear magnetic resonance evidence for structural order in extruded phosphate glasses. J. Non-Cryst. Solids **241** (1998) p. 204–207.

[7] Simmons, J. H.; Ochoa, R.; Simmons, K. D. et al.: Non-Newtonian viscous flow in soda-lime–silica glass at forming and annealing temperatures. J. Non-Cryst. Solids **105** (1988) p. 313–322.

[8] Pevzner, B. Z.; Klyuev, V. P.: Rheological properties of partially crystalline lithium disilicate melts. (Orig. Russ.) In: Mazurin, O. V. (ed.): Proc. 15th International Congress on Glass, Leningrad 1989. Vol. 2b Leningrad: Nauka, 1989. p. 277–280.

[9] Gutzow, I.; Rüssel, C.; Durschang, B.: Crystallization of glass forming melts under hydrostatic pressure and shear stress. Pt. 2. Flow induced melt crystallization: A new method of nucleation catalysis. J. Mater. Sci. **32** (1997) p. 5405–5411.

[10] Li, J. H.; Uhlmann, D. R.: The flow of glass at high stress levels. Pt. 1. Non-Newtonian behavior of homogeneous 0.08 $Rb_2O \cdot 0.92\ SiO_2$, glasses. J. Non-Cryst. Solids **3** (1970) p. 127–147.

[11] Manns, P.; Brückner, R.: Non-Newtonian flow behaviour of a soda-lime silicate glass at high deformation rates. Glastech. Ber. **61** (1988) no. 2, p. 46–56.

[12] Yue, Y.; Brückner, R.: A new description and interpretation of the flow behaviour of glass forming melts. J. Non-Cryst. Solids **180** (1994) p. 66–79.

[13] Habeck, A.; Brückner, R.: Direct connection between anisotropic optical properties, polarizability and rheological behaviour of single-phase glass melts. J. Non-Cryst. Solids **162** (1993) p. 225–236.

[14] Brückner, R.; Yue, Y.: Non-Newtonian flow behaviour of glass melts as a consequence of viscoelasticity and anisotropic flow. J. Non-Cryst. Solids **175** (1994) p. 118–128.

[15] Deubener, J.; Brückner, R.: Influence of nucleation and crystallisation on the rheological properties of lithium disilicate melt. J. Non-Cryst. Solids **209** (1997) p. 96–111.

[16] Brückner, R.: Anisotropic glasses and glass melts – a survey. Glastech. Ber. Glass Sci. Technol. **69** (1996) no. 12, p. 396–411.

[17] Yue, Y.; Carl, G.; Rüssel, C.: Rheological properties of calcium metaphosphate melts during extrusion. Glastech. Ber. Glass Sci. Technol. **72** (1999) no. 3, p. 67–75.

[18] Yue, Y.; Moisescu, C.; Carl, G. et al.: Influence of suspended iso- and anisometric crystals on the flow behaviour of fluoroapatite glass melts during extrusion. Phys. Chem. Glasses **40** (1999) no. 5, p. 243–247.

[19] Roeder, E.: Extrusion of glass. J. Non-Cryst. Solids **5** (1970/71) p. 377–388.

[20] Troost, A.: Zur elementaren Theorie des axialsymmetrischen Vorwärtsstrangpressens; Ermittlung der Umformgeometrie und des Kraftbedarfs durch Variationsrechnung. Arch. Eisenhüttenwes. **44** (1973) no. 4, p. 315–320.

[21] Cox, G.; Roeder, E.: Kraftbedarf und Austrittgeschwindigkeit beim Strangpressen einer Alkali-Kalksilicatglasschmelze. T. 2. Umformvorgänge innerhalb der Umformzone und des Blockaufnehmers. Glastech. Ber. **57** (1984) no. 8, p. 208–213.

[22] Gutzow, I.; Schmelzer, J.: The vitreous state. Thermodynamics, structure, rheology, and crystallization. Berlin (et al.): Springer, 1995. p. 371.

0600P003

Address of the authors:

C. Moisescu, G. Carl, C. Rüssel
Otto-Schott-Institut für Glaschemie
Friedrich-Schiller-Universität Jena
Fraunhoferstr. 6
D-07743 Jena